Experimental Floating Electrode Electric Curtain Evaluation to Contain Airborne Particles Resulting From the Paper Industrial Manipulation

JOAN J. GARCÍA-GARCÍA [ID], (Member, IEEE)

Grupo de Aplicaciones Electro-Magnéticas Aplicadas (GAEMI), Departament d'Enginyeria Electrònica, Universitat Autònoma de Barcelola, 08193 Barcelona, Spain

e-mail: joan.garcia@uab.es

ABSTRACT This paper describes the design, fabrication and characterization of a three phase floating electrodes electroportation system for dust confinement, compatible with industrial optical quality control systems. The proposed Floating Electrode Electronic Curtain (FE-EC) is composed of floating parallel wire electrodes framed by a two-layer PCB. The floating electrodes are connected to one of the synchronized three channels to generate an electric field traveling wave. The separation between the floating wire electrodes has been determined by minimizing the number of trajectories crossing the FE-EC using a numerical simulation tool. It is shown that the effect of the FE-EC in the luminosity of an industrial led luminaire can be compensated by an 1% increment in the led supply voltage. The performance of the fabricated FE-EC prototype is experimentally quantified, showing efficiencies higher than 95% in simulated relevant conditions.

INDEX TERMS Airborne dust control, dielectrophoretic force, electric curtain.

I. INTRODUCTION

The electrodynamic screen concept was introduced by F.B. Tatom [1] in 1967, and further developed and implemented by Masuda *et al.* at the Tokyo University in the 1970s [2]–[4]. Since then, electroportation based techniques have been used in a very wide application range, from solar cell cleaning [5]–[10] to radioactive dust manipulation in fusion reactors [11], [12], microfluidics [13], [14] , control of bubbles in dielectric liquids [15], sorting and manipulating particles by size [16]–[19], cell transport in liquid medium [20], [21] or dust reduction in professional environments in the so called electrostatic precipitators [18], [22], [23]. The electrostatic precipitator operation relays in the natural or induced particle charge and has been consolidated as an excellent method for the removal of particles greater than 1 μm suspended in gases, constituting the most commonly technology to clean the emission in power plants [23]. The present work has the practical objective to develop a Floating Electrodes-Electric Curtain (FE-EC) to

The associate editor coordinating the review of this manuscript and approving it for publication was Shuaihu Li [ID].

contain airborne suspended paper dust particles in industrial environments to protect delicate equipment, i.e. the elements of an optical quality control system. The FE-EC is based on the so called dielectrophoretic (DEP) force. The DEP force term was introduced in 1951 by H. A. Pohl [24] and constitute the seed of considerable research activity [25]. The utilization of DEP forces to filter and precipitate airborne particles, has been previously reported in the literature [26], [27]. However, this is the first time that the technique is applied to generate a Floating Electrode Curtain to content suspended industrial paper dust. The dynamic of small particles interacting with non-homogeneous electric fields is a major problem that depends in a complex way of parameters like the particle mass, size, permittivity and charge of the target particles as well as the field distribution [28]–[34]. The electroportation design proposed in this work is based on the three phase interdigital wire electrodes scheme, common in the solar cell cleaning systems, with the particularity that the wire electrodes are floating (and the air can freely circulate through the barrier). The applied voltage pulses in the FE-EC are low frequency asymmetric pulses up to 2.5 kV which generate a single front in the non-homogeneous electric field

traveling wave. A functional FE-EC prototype has been designed, fabricated and tested. To quantify the effect of the FE-EC as dust barrier, the number of particles crossing the FE-EC with and without the effect of the electric pulses traveling across the wire electrodes has been compared. Dust samples used to characterize the FE-EC, are composed of cellulose agglomerates fragments, kaolin and other paper chemical additives mixed with arabic gum 30 μm average size spheres formed in air suspension as a result of industrial processes. The developed prototype has been designed to safely operate up to 4.4 kV DC voltages. 3D CST-Particle Studio software has been used as numerical tool to set the parameters that minimize the number of particle trajectories crossing the FE-EC. This numerical optimization tool avoids dealing with the complexity of the details of an analytical theoretical framework, simplifying the design process. The FE-EC prototype has shown efficiencies greater than 95% acting as dust containing barrier. The light transparency of the FE-EC has been characterized to check the compatibility of the prototype with industrial led luminaries for the optical quality control systems.

II. THEORETICAL FRAMEWORK
The applied force on a homogeneous spherical particle in presence of an electric field has the four main contributions described in Equation (1) [19]

$$\vec{F} = m_p \cdot \vec{g} + q_s \vec{E} + 6\pi \xi R_p \vec{U} + 2\pi R_p^3 \frac{\varepsilon_p - \varepsilon_0}{\varepsilon_p + 2 \cdot \varepsilon_0} \vec{\nabla} |E|^2 \quad (1)$$

where mp is the particle mass, $\vec{g}$ the gravity constant (9.8 m/s2), qs, the particle charge, ξ is the kinematic air viscosity (between $1.71 \cdot 10\text{-}5$ Pa $\cdot$ s and $1.95 \cdot 10\text{-}5$ Pa $\cdot$ s), $\vec{U}$ is the particle velocity, Rp the particle radius, ep the particle dielectric permittivity, eo the free space permittivity ($8.9 \cdot 10\text{-}12$ F/m) and $\vec{E}$ is the applied electric field.

The consideration of all the terms in equation (1) in the analysis of particle's dynamics when a spatially non-homogeneous electric field is applied, leads to complex, and even chaotic trajectories [28], [32]. However, for practical applications only the conditions to establish an effective drift velocity to the dust particles are necessary rather than the analytical details of the trajectories. Numerical methods are commonly used to deal with the complexity of the problem [35]–[37]. Considering the typical intrinsic dust particle charge reported in the literature [10], [27], [30], it can be shown that the dominant term in the equation (1) for voltages in the range of kV and for electrode distances <1 mm is the DEP force, being the rest of the terms orders of magnitude lower. This dominant term is proportional to the electric field gradient and the permittivity difference between the particle and the medium [38]. In the case of air background, the particles tend to move towards the more intense electric field regions from the lower electric field regions [18] making possible the design of electric curtains for non-charged dielectric particles, Moreover, it has been shown that the DEP forces contribute significantly in the particle's movement especially during the transient that lead to the establishment of the electrostatic field distribution [39], [40]. The proposed FE-EC takes advantage of this intense initial transient effect in combination with the traveling wave effect to avoid that the trajectories of the airborne particles cross the plane determined by the FE-EC floating wire electrodes.

III. DUST PARTICLES DESCRIPTION
The industrial paper manipulation utilizes processes in which the paper webs circulate at rates in the order of 100 m per minute or even higher, inevitably generating the expulsion of particles to the ambient. Furthermore, the utilization of volatile chemical products like ink, paper chemical additives or other substances produce suspended micro-precipitates that contribute to the airborne dust. Real time quality controls based on optical systems are commonly used to monitor the industrial paper processes requiring maintenance tasks due to the dust accumulation that hinder the production. The objective of this work is the design and fabrication of a dust containment barrier that minimizes the dust accumulation in the luminaires of the optical quality control systems. The FE-EC to develop should be effective for air suspended non-charged dielectric particles with sizes ranging from a few microns to 30 μm. Fig. 1 shows two different examples of this target dust. Fig. 1 (a) sample is composed of small and irregular particles mainly formed by agglomerations of paper loads and cellulose fibers with an average density of 1.5 gr/cm^3 with average dimensions lower than 10 μm.

Particles around 0.5 μm are expected to be formed by crystals and precipitators of chemistry substances used to control color, flexibility and other properties of the paper. In this case, the mean size is below 10 μm, although larger agglomerates including cellulose fiber can be found.

Fig. 1 (b) shows a completely different dust type mainly formed by 30 μm average diameter spheres of arabic gum which typical density is 0.64 gr/cm^3. The overall average expected mass of the particles is 0.014 μgr. The dust to contain may be a mix between typically 2 μm crystals of chemical precipitates, 10 μm cellulose particles, and 30 μm average diameter arabic gum spheres.

IV. PROPOSED FE-EC DESIGN DESCRIPTION
The structure of the proposed FE-EC is an interdigital three-phase square pulses scheme, which has already tested and successfully applied in other electronic curtain designs [31], [32]. Unlike of the electric curtains in other works, the electrode wires of the proposed FE-EC are floating, in such a way that the air and light can flow though the electric curtain electrode wires. The effect of the electronic curtain is to modify the trajectory of the flying particles in such a way that the plain containing the floating electrodes becomes a barrier for the suspended dust particles.

The physical structure of the curtains consists on a standard 2-layer FR4 PCB frame containing the interconnection matrix to connect each floating wire electrode with one of the three synchronized channels. The floating electrodes are
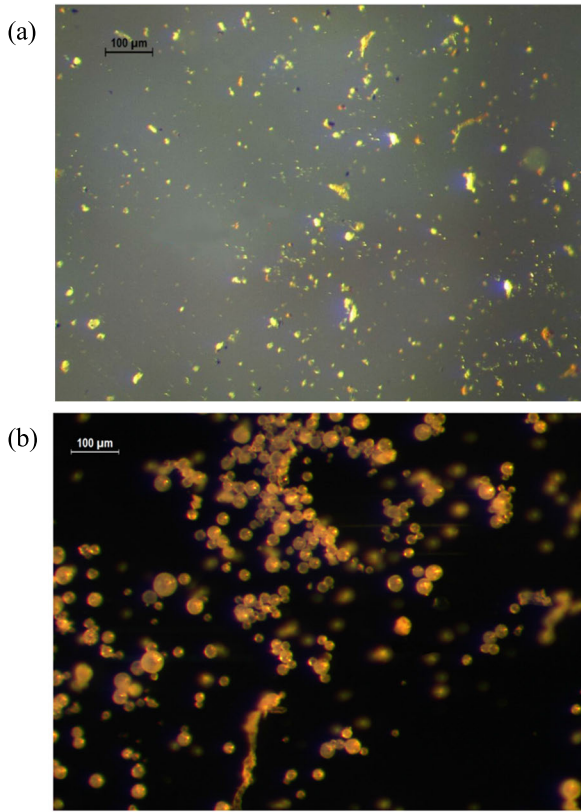
FIGURE 1. Microscope images of two different dust samples. a) dust composed by cellulose fibers, kaolin and other chemical additives agglomerations with 10 μm average dimensions. b) dust mainly composed by 30 μm average radius spheres of arabic gum.

FIGURE 2. Details of the three-phase structure. (a) Layout of the TCE structure showing the top (green lines), bottom (red lines) metallic layers and the holes (blue) in the PCB, and the main dimensions. 20.124 mm width of the floating electrodes windows, 1 mm minimal separation between electrode wires PCB holes. (b) picture showing the top of the FE-EC before soldering and passivate.

implemented using 150 μm (38 SWG) copper wires with an enamel coating resistant up to 400 °C and 1.5 kV$_{\text{RMS}}$ electric breakdown. This insulation level combined with the 3 kV/mm air breakdown ratio provides a safe operability up to 4.5 kV DC in the floating electrodes area when using an inter-electrode distance of 0.8 mm. The PCB interconnection matrix structure is passivated using the encapsulation Epoxy ER22193SL after the soldering process, guaranteeing an electrical strength of 12 kV per mm in the PCB frame area.

The three channels of the proposed FE-EC are excited with square pulses out of phase to generate an electric field distribution (see Fig.3), traveling perpendicularly to the parallel wire electrodes. After several tests, a low operating frequency of 10 Hz has proved to be the most effective for the tested dust samples. The FE-EC channels have been implemented by synchronizing three Advanced Energy Ultravolt 4HVA precision high voltage amplifier which offers rising times for the pulses < 1 ms.

As it has been said, to deal with the complexity of the electroportation problem is common the utilization of numerical tools to describe the interaction between the dielectric particles and the spatial inhomogeneous electric fields [32], [34], [35]. In our case, the full 3D electromagnetic simulation software CST Studio has been used to visualize
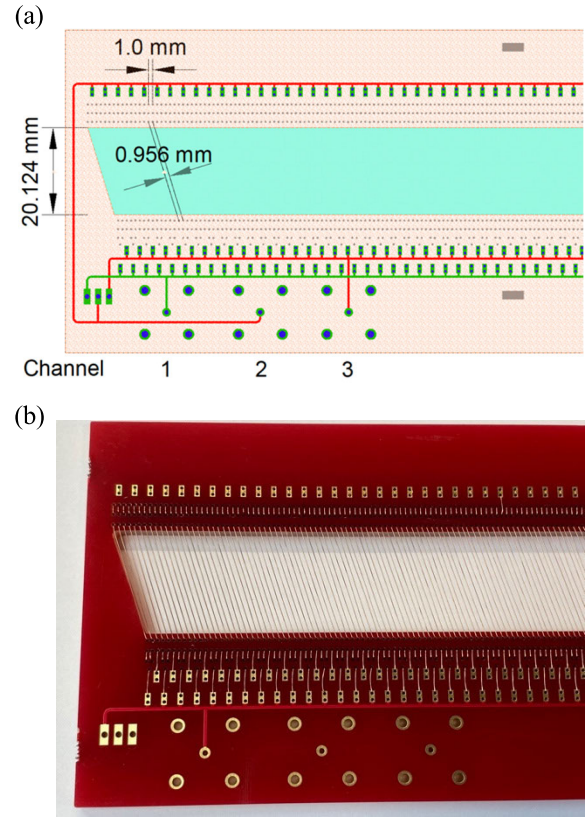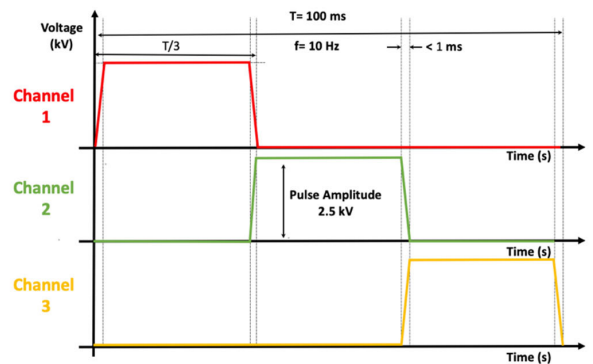

FIGURE 3. Electric scheme of the electric curtain three channel exciting pulses. The rise, hold and down time is T/3 where T is a period of 0.1 s corresponding to 10 Hz. The nominal pulse value is set equal for the three channels in values between 0 kV and 2.4 kV. This value is surpassed in the rising flank in a 15% overshoot (<1ms).

the 3D spatial field distribution generated by the electrodes (Fig. 4 (a)) and to design a proper insulation strategy to avoid spark discharges produced by electrical break-down. On the other hand, the CST-Particle Studio module has been used in a parametric study that allows to explore the robustness of the system. Fig. 4 (b) shows the trajectories of
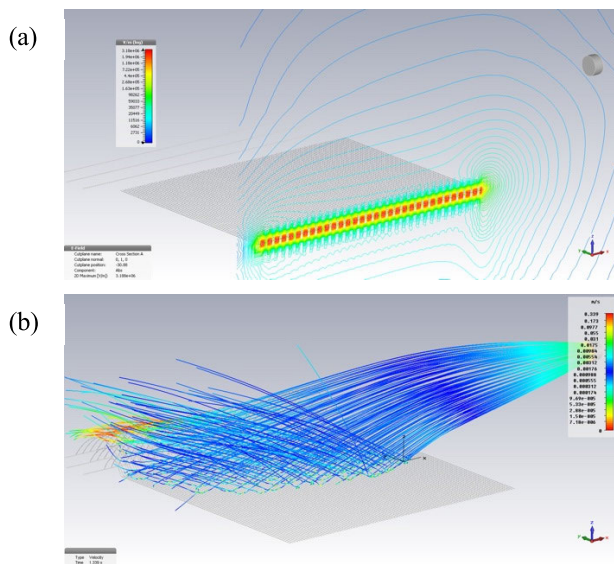
FIGURE 4. (a) 3D absolute electric field isolines over a plane perpendicular to the plane defined by the parallel floating electrodes. (b) simulated particle's trajectories after the optimization process in which the plane defined by the floating parallel wire electrodes (in grey) defines an effective barrier for the particles.

FIGURE 5. Effect of the electric curtain floating electrode wires in the luminosity of a led industrial illumination system for different led supply voltages. In the inside is depicted the reduction percentage of the luminosity by the effect of the FE-EC screening. The voltage increment to compensate the screening is <1% in all the points tested.

FIGURE 6. Picture of the experimental setup used to quantify the effect of the FE-EC as dust barrier. The FE-EC acts as a vertical boundary of the confining the Airborne atmosphere. The FE-EC removed dust is deposited in the bottom of the volume.

particles interacting with the electric field distribution shown in Fig. 4 (a). The parametric analysis points out that for 150 μm wires with 0.8 mm separation distance and three phases with 2.4 kV the trajectories of for particles in the range between 10^{-12} gr and 10^{-11}gr does not cross the FE-EC plain (see Fig. 4 (b)). The particle charge parameter for the simulations, has been estimated using the dielectric saturation charge expression $Q_{sat} = 12\pi\varepsilon_o E_o R_P^2$ [25], obtaining $3.0 \cdot 10^{-11}$ C in the case of the 30 μm gum arabic particles, $3.3 \cdot 10^{-12}$ for the 10 μm cellulose particles or $1.3 \cdot 10^{-13}$ C for the 2 μm kaolin precipitates.

To ensure the compatibility of the TE-EC prototype with the industrial optic quality control system, the effect of the parallel electrode wires on the luminosity of an industrial led luminaire has been quantized. The luminosity of the luminaire can be adjusted by the supply voltage being possible to operate in a range between 24 V and 28 V offering brightness between and 10 lx. The results in Fig. 5 show that the effect luminosity reduction introduced by the FE-EC is between 6.5% and 8%.

As can be observed in Fig.5, the light attenuation introduced by the FE-EC can be compensated with less than an 1% increment in the led supply voltage. This transparency level is important from a practical point of view to guarantee that the FE-EC compatibility with the industrial environment.

V. EXPERIMENTAL SETUP AND MEASUREMENTS

The effectivity of the proposed FE-EC as airborne dust barrier has been tested using the experimental setup showed in Fig. 6. The experimental setup aims to reproduce the operating conditions of an industrial led illumination system exposed to an atmosphere with dust in suspension. The dust
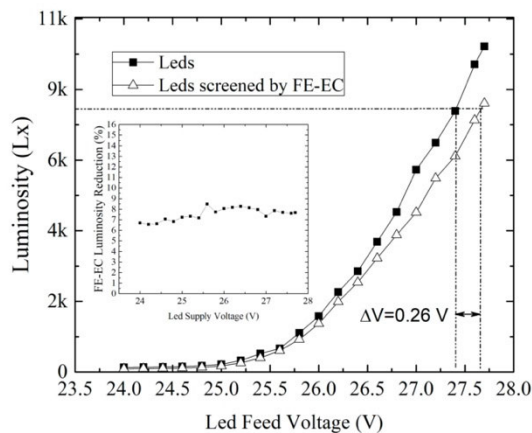
atmosphere is generated by a vibrating 50 μm sieve in the top of the confined volume. The electric curtain has been fixed perpendicular to the ground, limiting the confined volume containing the flying dust particles. The natural tendency of the dust particle is to fall and be spreader in the volume due to the air turbulences. The number of particles crossing the electric curtain are counted using a Fluke 985 Airborne Counter. This device requires a small and continuous air flux trough the internal sample reservoir where the particles are detected and counted using a laser sensor. As a consequence, the sensing process produces a small air flux through the electric curtain that favors the particle curtain permeability.

The effect of the electric curtain is quantified using the efficiency defined in Eq. 2. This efficiency figure is obtained by normalizing the number of particles crossing the FE-EC barrier in the case of non-active curtain (all channels set to 0 V pulses), with the number of particles detected when the curtain is active applying pulses with different amplitudes.

The airborne dust generated depends of the size of the dust particles, the air turbulences or the vibrating frequency of the sieve. In order to compare the FE-EC efficiency of different
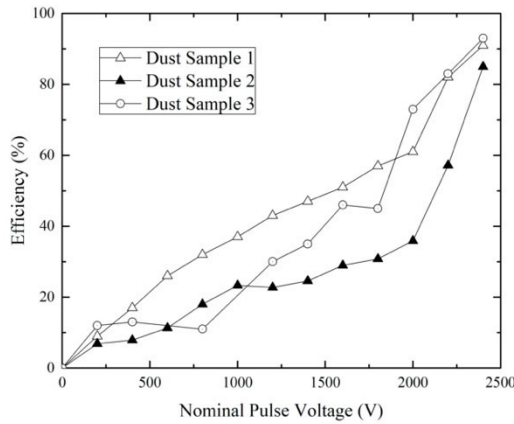
FIGURE 7. Effect of the amplitude of the pulses applied in the FL.EC barrier efficiency for three different industrial dust samples: sample 1: average 30 μm arabic gum spheres; sample 2: dust containing arabic gum spheres and paper dust; sample 3: paper dust sample.
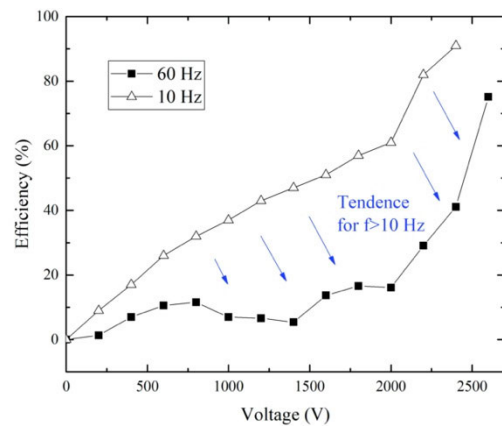

FIGURE 8. Efficiency tendency with the frequency increment for the Dust Sample 1with the frequency increment. Similar behavior is found for samples 2 and 3. No significant differences has been found for frequencies between 10 and 1 Hz.

samples and conditions, the measures are normalized, and the efficiency expressed in %.

$$\eta = 1 - \frac{\textit{Number of particles detected with the FE} - \textit{EC ON}}{\textit{Number of particles detected with the FE} - \textit{EC OFF}} \quad (2)$$

As it can be observed in Fig. 7 graph, the effectivity of the FE-EC as dust particle barrier reaches values greater than 95% for 2.6 kV amplitude pulses.

The results shown in Fig. 7 point out that the FE-EC is more efficient with the arabic gun 30 mm spherical particles (sample 1) for any voltages. The efficiency improvement beyond 2 kV observed in the tree analyzed samples, is attributable to the generation of real charge in the particles due to the effect of the intense electric fields in the FE-EC. However, more tests should be done to clarify this interpretation which are out of the scope of this work.

The optimum operating frequency depends on the mass and charge of the particles, as well as on the distance between the electrodes and the voltage difference between them. Fig. 8 illustrate the results of this experimental analysis in the case of the dust sample 1. Similar tendencies can be found for the rest of the analyzed samples.

VI. CONCLUSION

A dust container barrier based on a three Channels scheme FE-EC has been designed, fabricated and tested showing efficiencies up to 95% for 2.4 kV square pulses operating at 10 Hz.

The parallel floating electrodes constitute dust barrier transparent and permeable to air. Numerical tools have been used to set the minimal distance between electrodes to minimize the dust trajectories traveling through the FE-EC barrier. The FE-EC prototype has demonstrated to be more efficient containing dielectric particles with dimensions between 10 and 30 μm. The increment of the square pulse amplitude produces a clear increment of the efficiency, which is accentuated for voltages greater than 2 kV in all the evaluated samples. This effect is attributed to the polarization of the particles due to the intense electric fields produced. Work is in progress to analyze in detail this effect and to apply the technique industrially.

REFERENCES

[1] F. B. Tatom, V. Srepel, R. D. Johnson, N. A. Contaxes, J. G. Adams, H. Seaman, and B. L. Cline, "Lunar dust degradation effects and removal/prevention concepts," NASA, Washington, DC, USA, Tech. Rep. TR-792-207A, 1967.

[2] S. Masuda, K. Fujibayashi, and K. Ishida, "Electric curtain for repulsion, confinement, and transport of charged dust clouds," *Trans. Inst. Electr. Eng. Jpn.*, vol. 92-B, 1972.

[3] B. S. Masuda and Y. Matsumoto, "Theoretical characteristics of standing-wave electric curtains," *Electr. Eng. Jpn.*, vol. 1, pp. 7–71, Dec. 1973.

[4] S. Masuda and T. Kamimura, "Approximate methods for calculating a non-uniform travelling field," *J. Electrostatics*, vol. 1, no. 4, pp. 351–370, Nov. 1975.

[5] C. I. Calle, C. R. Buhler, J. L. McFall, and S. J. Snyder, "Particle removal by electrostatic and dielectrophoretic forces for dust control during lunar exploration missions," *J. Electrostatics*, vol. 67, nos. 2–3, pp. 89–92, May 2009.

[6] R. Sharma, C. A. Wyatt, J. Zhang, C. I. Calle, N. Mardesich, and M. K. Mazumder, "Experimental evaluation and analysis of electrodynamic screen as dust mitigation technology for future mars missions," *IEEE Trans. Ind. Appl.*, vol. 45, no. 2, pp. 591–596, May 2009.

[7] M. K. Mazumder, R. Sharma, A. S. Biris, J. Zhang, C. Calle, and M. Zahn, "Self-cleaning transparent dust shields for protecting solar pan and other devices," *Particulate Sci. Technol.*, vol. 25, no. 1, pp. 5–20, 2007.

[8] L. K. Verma, M. Sakhuja, J. Son, A. J. Danner, H. Yang, H. C. Zeng, and C. S. Bhatia, "Self-cleaning and antireflective packaging glass for solar modules," *Renewable Energy*, vol. 36, no. 9, pp. 2489–2493, 2011.

[9] A. Sayyah, D. R. Crowell, A. Raychowdhury, M. N. Horenstein, and M. K. Mazumder, "An experimental study on the characterization of electric charge in electrostatic dust removal," *J. Electrostatics*, vol. 87, pp. 173–179, Jun. 2017.

[10] H. Kawamoto and T. Shibata, "Electrostatic cleaning system for removal of sand from solar panels," *J. Electrostatics*, vol. 73, pp. 65–70, Feb. 2015.

[11] M. Onozuka, Y. Ueda, Y. Oda, K. Takahashi, Y. Seki, I. Aoki, S. Ueda, and R. Kurihara, "Development of dust removal system using static electricity for fusion experimental reactors," *J. Nucl. Sci. Technol.*, vol. 34, no. 11, pp. 1031–1038, Nov. 1997.

[12] F. Q. Friesen, B. John, C. H. Skinner, A. L. Roquemore, and C. I. Calle, "Evaluation of an electrostatic dust removal system with potential application in next-step fusion devices," *Rev. Sci. Instrum.*, vol. 82, no. 5, May 2011, Art. no. 053502, doi: 10.1063/1.3587619.

[13] H. Yang, H. Jiang, D. Shang, A. Ramos, and P. Garcia-Sanchez, "Experiments on traveling-wave electroosmosis: Effect of electrolyte conductivity," *IEEE Trans. Dielectr. Electr. Insul.*, vol. 16, no. 2, pp. 417–423, Apr. 2009.

[14] P.-W. Yen, S.-C. Lin, Y.-C. Huang, Y.-J. Huang, Y.-C. Tung, S.-S. Lu, and C.-T. Lin, "A low-power CMOS microfluidic pump based on travelling-wave electroosmosis for diluted serum pumping," *Sci. Rep.*, vol. 9, no. 1, Dec. 2019, Art. no. 14794, doi: 10.1038/s41598-019-51464-7.

[15] M. Aoyama, T. Oda, M. Ogihara, Y. Ikegami, and S. Masuda, "Electro-dynamical control of bubbles in dielectric liquids using a non-uniform traveling field," *J. Electrostat.*, vol. 30, pp. 247–258, 1993.

[16] H. Kawamoto, "Some techniques on electrostatic separation of particle size utilizing electrostatic traveling-wave field," *J. Electrostat*, vol. 66, pp. 220–222, 2008.

[17] Y. Zhao, U.-C. Yi, and S. K. Cho, "Microparticle concentration and separation by traveling-wave dielectrophoresis (twDEP) for digital microfluidics," *J. Microelectromech. Syst.*, vol. 16, no. 6, pp. 1472–1481, Dec. 2007.

[18] A. Belgacem, A. Tilmatine, Y. Bellebna, F. Miloua, N. Zouzou, and L. Dascalescu, "Experimental analysis of the transport and the separation of plastic and metal micronized particles using travelling waves conveyor," *IEEE Trans. Dielectr. Electr. Insul.*, vol. 25, no. 2, pp. 435–440, Apr. 2018.

[19] M. Adachi, H. Moroka, H. Kawamoto, S. Wakabayashi, and T. Hoshino, "Particle-size sorting system of lunar regolith using electrostatic traveling wave," *J. Electrostatics*, vol. 89, pp. 69–76, Oct. 2017.

[20] S. Masuda, M. Washizu, and I. Kawabata, "Movement of blood cells in liquid by nonuniform traveling field," *IEEE Trans. Ind. Appl.*, vol. 24, no. 2, pp. 217–222, Mar. 1988.

[21] W. M. Arnold and G. Fuhr, "Increasing the permittivity and conductivity of cellular electromanipulation media," in *Proc. IEEE Ind. Appl. Soc. Annu. Meeting*, Dec. 1994, pp. 1470–1476.

[22] A. Mizuno, "Electrostatic precipitation," *IEEE Trans. Dielectr. Electr. Insul.*, vol. 7, no. 5, pp. 615–624, Oct. 2000.

[23] A. Jaworek, A. Marchewicz, A. T. Sobczyk, A. Krupta, and T. Czech, "Two-stage precipitators for the reduction of PM2.5 particle emission," *Prog. Energy Combustion Sci.*, vol. 67, pp. 233, Apr. 2018.

[24] H. A. Pohl, "The motion and precipitation of suspensoids in divergent electric fields," *J. Appl. Phys.*, vol. 22, no. 7, pp. 869–871, Jul. 1951.

[25] R. Pethig, "Dielectrophoresis: Status of the theory, technology, and applications," *Biomicrofluidics*, vol. 4, Apr. 2010, Art. no. 022811.

[26] J. D. Duff, "Dielectrophoretic precipitation of airborne particles," Ph.D. dissertation, 2013, Paper 376, doi: 10.18297/etd/376.

[27] H. Kawamoto and M. Adachi, "Electrostatic particle-size classification of lunar regolith for *in-situ* resource utilization," in *Proc. 7th Symp. Space Resource Utilization*, National Harbor, MD, USA, 2014, pp. 1–8.

[28] G. Liu and J. S. Marshall, "Particle transport by standing waves on an electric curtain," *J. Electrostatics*, vol. 68, no. 4, pp. 289–298, Aug. 2010.

[29] C. E. P. K. Johnson Srirama, R. Sharma, K. Pruessner, J. Zhang, and M. K. Mazumder, "Effect of particle size distribution on the performance of electrodynamic screens," in *Proc. IEEE Conf. Ind. Appl.*, Oct. 2005, pp. 341–345.

[30] H. Kawamoto, K. Seki, and N. Kuromiya, "Mechanism of traveling-wave transport of particles," *J. Phys.*, vol. 39, pp. 1249–1256, Apr. 2006.

[31] M. N. Horenstein, M. K. Mazumder, R. C. Sumner, J. Stark, T. Abuhamed, and R. Boxman, "Modeling of trajectories in an electrodynamic screen for obtaining maximum particle removal efficiency," *IEEE Trans. Ind. Appl.*, vol. 49, no. 2, pp. 707–713, Mar. 2013.

[32] M. N. Horenstein, M. Mazumder, and R. C. Sumner, "Predicting particle trajectories on an electrodynamic screen—Theory and experiment," *J. Electrostatics*, vol. 71, no. 3, pp. 185–188, Jun. 2013.

[33] J. R. Melcher, E. P. Warren, and R. H. Kotwal, "Theory for finite-phase traveling-wave boundary-guided transport of triboelectrified particles," *IEEE Trans. Ind. Appl.*, vol. 25, no. 5, pp. 949–955, Sep. 1989.

[34] J. R. Melcher, E. P. Warren, and R. H. Kotwal, "Traveling-wave delivery of single-component developer," *IEEE Trans. Ind. Appl.*, vol. 25, no. 5, pp. 956–961, Sep. 1989.

[35] N. G. Green, A. Ramos, and H. Morgan, "Numerical solution of the dielectrophoretic and travelling wave forces for interdigitated electrode arrays using the finite element method," *J. Electrostatics*, vol. 56, no. 2, pp. 235–254, Sep. 2002.

[36] A. Zouaghi, N. Zouzou, and L. Dascalescu, "Effect of travelling wave electric field on fine particles motion on an electrodynamic board," in *Proc. IEEE Ind. Appl. Soc. Annu. Meeting*, Oct. 2017, pp. 1–9.

[37] E. Amah, M. Janjua, and P. Singh, "Direct numerical simulation of particles in spatially varying electric fields," *Fluids*, vol. 3, p. 52, Sep. 2018, doi: 10.3390/fluids3030052.

[38] M. Abraham, *The Classical Theory of Electricity and Magnetism*. New York, NY, USA: Hafner, 1932.

[39] H. A. Pohl, *Dielectrophoresis: The Behavior of Neutral Matter in Nonuniform Electric Fields*, vol. 80. Cambridge, U.K.: Cambridge Univ. Press, 1978.

[40] T. B. Jones, *Electromechanics of Particles*. Cambridge, U.K.: Cambridge Univ. Press, 1995.

• • •